*Optica Applicata, Vol. XXIX, No. 1–2, 1999*

# Highly-birefringent elliptical structures

ZYGMUNT KRASIŃSKI, ADAM MAJEWSKI

Institute of Electronic Systems, Warsaw University of Technology, ul. Nowowiejska 15/19, 00–665 Warszawa, Poland.

TAKASHI HINATA

College of Science and Technology, Nihon University, 1–8 Kanda, Surugadai, Chiyoda-ku, Tokyo 101, Japan.

An analysis of isotropic multi-step fiber structures with elliptical geometry, in particular, the fiber structures which provide the large value of the birefringence, is presented. The multi-layer confocal-elliptical fibers can be analyzed by the exact analytical method with Mathieu function expansions. In that group of fibers, the *W*-profile elliptical fiber provides the largest value of the birefringence. In order to investigate the three-layer elliptical fibers with layers of any ellipticity we apply the improved point-matching method with Mathieu function expansions. It was found that the highly-birefringent fibers with hollow layers outside an elliptical core can be suitable for the single-mode single-polarization transmission. Numerical resutls are presented for the silica fibers doped $GeO_2$ and F, respectively. The results obtained are of the practical value and can be used directly in designing the elliptical fibers with large value of the birefringence.

## 1. Introduction

The elliptical fiber is defined as a fiber with the core of elliptical cross-section. Due to the cross-section asymmetry, in the elliptical fiber two orthogonally polarized modes of different values of the propagation constants can be propagated. Therefore the elliptical fibers can preserve the polarization of guided mode and they play an important role in the domain of the optical fiber technology, especially, optical fiber sensing systems. The ability of a fiber to preserve the polarization becomes greater as the modal birefringence $B$ of a fiber is increasing, where $B$ is defined as

$$B = |\Delta\beta|/k \tag{1}$$

where $\Delta\beta$ is the difference of propagation constants of the odd and even fundamental modes, and $k$ – the wave number of a free space.

In a real fiber structure with large value of birefringence, *i.e.*, for the case of $B$ larger than $10^{-5}$, accidental $B$ fluctuations caused by heterogeneity of the core and mechanical stresses do not have an effect on the light polarization.

The first paper on elliptical fibers appeared in 1961 [1], while the theoretical study on the step-index dielectric-elliptical fiber was published by YEH in 1962 [2]. He derived the characteristic equations for odd and even modes and presented

selected propagation characteristics for the fundamental modes of the fiber. Yeh has also derived the characteristic equations in a simplified form in case of the weakly guiding fibers [3] and investigated attenuation in elliptical fiber [4]. Single-mode optical fibers with elliptical core have been shown to preserve the polarization [5]. RENGARAJAN and LEWIS analyzed the first higher-mode cut-off parameter of the step-index elliptical fiber [6]. The results of studies have confirmed that a value of $B$ possible to obtain in the case of step-index elliptical fibers of low-dispersion is not so large (about $10^{-5}$).

The analysis of elliptical dielectric tube waveguides [7] was modified to study the propagation characteristics of three-layer elliptical fibers [8]. Among that group of fibers the $W$-type confocal-elliptical fiber was proposed for polarization-maintaining and low-dispersion applications [8], [9]. In order to investigate the $W$-type elliptical fibers with layers of any ellipticity the authors proposed the improved point -matching method (IPMM) with Mathieu function expansion [10]. In our IPMM, unlike in the previously reported methods [11], [12], high computational accuracy was chieved even in the case of fibers with layers of larger ellipticity. It was found that the fibers with hollow layers outside an elliptical core can provide the large value of birefringence ($B > 10^{-3}$) and they can be suitable for the single-mode single-polarization transmission [13].

The subject of analysis are isotropic multi-step optical-fiber structures with elliptical geometry, in particular, the fiber structures which provide the large value of the birefringence.

The software to calculate the Mathieu functions was prepared by the authors. Numerical results of the propagation and dispersion characteristics, modal birefringence and cut-off conditions for the selected fiber structures are presented. The birefringence that arises from stress is assumed to be neglected in this paper.

## 2. Confocal-elliptical fibers

### 2.1. Step-index elliptical fibers

In an analysis of the step-index elliptical fibers the elliptical coordinates $(\xi, \eta, z)$ are used. The cross-section of the step-index elliptical fiber is shown in Fig. 1. It is assumed that the core is an infinitely long dielectric cylinder of an elliptical cross-section and a permittivity $\varepsilon_1$. Outside of the surface $\xi = \xi_0$ we have an infinite dielectric medium of permittivity $\varepsilon_2$, the so-called cladding, where $\varepsilon_1 > \varepsilon_2$.

We assume that the core and the cladding are isotropic, perfectly transparent for the light and their magnetic permeability is equal to the magnetic permeability of the free space $\mu_0$.

We shall confine our treatment to harmonic waves propagating along the positive $z$ axis. Therefore, the time $t$ and $z$ dependence of $e^{j(\omega t - \beta z)}$ for all field components is assumed, where $\omega = 2\pi f$, $f$ is frequency and $\beta$ is propagation constant.

The wave equation in the elliptical coordinates system has the form:

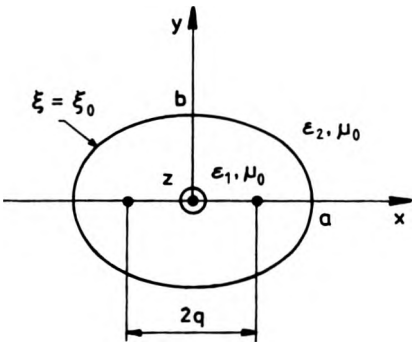


Fig. 1. Cross-section of step-index elliptical fiber: $a = q\,\mathrm{ch}\,\xi_0$ – semi-major axis of the ellipse, $b = q\,\mathrm{sh}\,\xi_0$ – semi-minor axis of the ellipse, $q$ – semi-focal length.

$$\frac{\partial^2 \Phi_z}{\partial \xi^2} + \frac{\partial^2 \Phi}{\partial \eta^2} + \chi^2 q^2 (\mathrm{ch}^2 \xi - \cos^2 \eta) \Phi_z = 0 \tag{2}$$

where $\Phi_z = \{E_z, H_z\}$, $E_z$ and $H_z$ are the axial electric and magnetic field components, respectively, $\chi^2 = k_i^2 - \beta^2$, $k_i^2 = \omega^2 \varepsilon_i \mu_0$, $i = \{1, 2\}$.

Using the method of separation of variables we can write that

$$\Phi_z = f(\xi) g(\eta) \tag{3}$$

where $f(\xi)$ – function of $\xi$, $g(\eta)$ – function of $\eta$. Therefore, the functions $f$ and $g$ are solutions of the equations [9]:

$$\frac{\partial^2 g}{\partial \eta^2} + [b(s) - s \cos^2 \eta] g = 0, \tag{4}$$

$$\frac{\partial^2 f}{\partial \xi^2} - [b(s) - s\,\mathrm{ch}^2 \xi] f = 0, \tag{5}$$

where $s = \chi^2 q^2$, $b(s)$ is the eigenvalue that is independent of $\xi$ and $\eta$.

Equations (4) and (5) are known as the Mathieu equation and modified Mathieu equation, respectively. Solutions of Eq. (4) have the form of the even and odd Mathieu functions of the first kind denoted by ce and se, respectively. In the case of Eq. (5), we have the modified Mathieu functions of the first kind: even – Ce and odd – Se, of the second kind: even – Fek and odd – Gek and of the third kind: even – Fey and odd – Gey, respectively. The Mathieu functions and modifies Mathieu functions are also known as the functions of hyperbolic and elliptic cylinders, respectively. Relations to calculate the Mathieu functions are given in [14], [15].

*Modes of the elliptical fiber*

Unlike the circular fiber, the elliptical fiber guides only the hybrid modes. In this case the modes TE ($E_z = 0$, $H_z \neq 0$) and TM ($H_z = 0$, $E_z \neq 0$) do not exist. Due to the asymmetry of the elliptical cylinder, it is possible to have two orientations of field configurations. Consequently, there are odd and even hybrid modes. The odd modes

are denoted by ${}_oHE_{mp}$, ${}_oEH_{mp}$ [2] or $HE_{1mp}$, $EH_{1mp}$ [16], where $m$ and $p$ are azimuthal and radial mode numbers, respectively. For HE and EH hybrid modes the axial components ratio of the electric and magnetic field ratio is positive and negative, respectively. In the case of the odd fundamental mode ${}_oHE_{11}$, electric field lines in the center of the fiber are perpendicular to the minor axis of the ellipse (Fig. 2a).

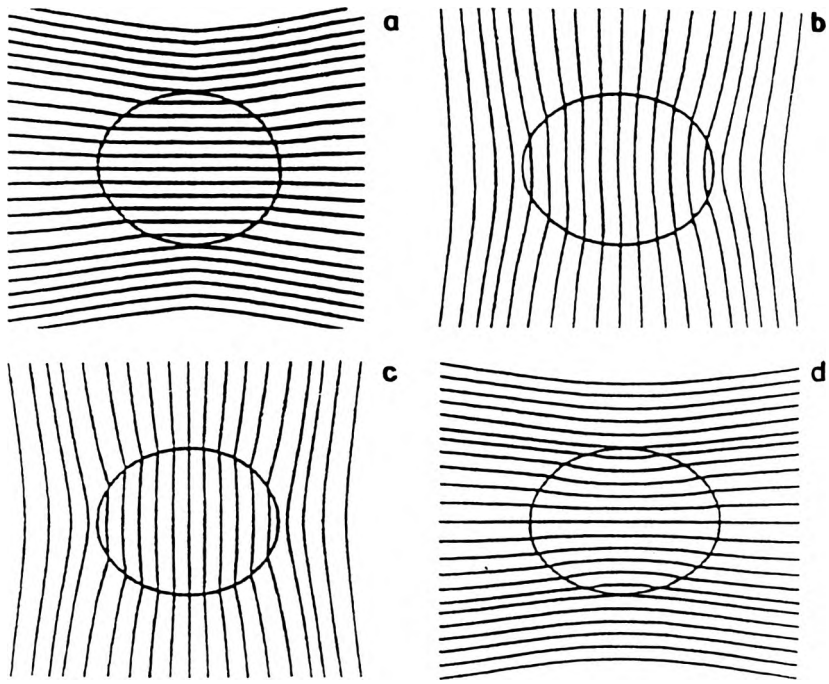


Fig. 2. Transverse electric and magnetic field lines of step-index elliptical fiber: the odd fundamental mode ${}_oHE_{11}$ (a — $E$ field, b — $H$ field) and the even fundamental mode ${}_eHE_{11}$ (c — $E$ field, d — $H$ field) for $b/a = 0.75$, $\Delta = 0.4$.

The even modes are denoted by ${}_eHE_{mp}$, ${}_eEH_{mp}$ [2] or $HE_{\perp mp}$, $EH_{\perp mp}$ [16]. In the case of the even fundamental mode ${}_eHE_{11}$, the electric field lines at the center of the fiber are perpendicular to the major axis of the ellipse (Fig. 2c).

The transverse electric and magnetic field configuration of the fundamental modes ${}_oHE_{11}$ and ${}_eHE_{11}$, as shown in Fig. 2, tend to the field configuration of the circular $HE_{11}$ mode when the ellipticity tends to zero [17]. The transverse electric and magnetic field configuration of the higher-order modes are presented in [9].

The axial magnetic and electric fields of an odd wave are represented by odd and even Mathieu functions, respectively, while those of an even wave by even and odd Mathieu functions, respectively.

*Odd ${}_oHE_{mp}$ and ${}_oEH_{mp}$ modes*

The appropriate solutions of Eq. (2) for the odd modes of the step-index fiber are as follows [9]:

$$H_{z1} = \sum_{m=1}^{\infty} C_m \mathrm{Se}_m(\xi, \gamma_1^2)\,\mathrm{se}_m(\eta, \gamma_1^2),$$
$$E_{z1} = \sum_{m=0}^{\infty} D_m \mathrm{Ce}_m(\xi, \gamma_1^2)\,\mathrm{ce}_m(\eta, \gamma_1^2), \tag{6}$$

for the core ($0 \leqslant \xi \leqslant \xi_0$) and

$$H_{z2} = \sum_{r=1}^{\infty} G_r \mathrm{Gek}_r(\xi, \gamma_2^2)\,\mathrm{se}_r(\eta, \gamma_2^2),$$
$$E_{z2} = \sum_{r=0}^{\infty} F_r \mathrm{Fek}_r(\xi, \gamma_2^2)\,\mathrm{ce}_r(\eta, \gamma_2^2), \tag{7}$$

for the cladding ($\xi_0 \leqslant \xi \leqslant \infty$), where: $\gamma_1^2 = (k_1^2 - \beta^2)q^2/4$, $\gamma_2^2 = (k_2^2 - \beta^2)q^2/4$, $k_1^2 = \omega^2 \mu_0 \varepsilon_1$, $k_2^2 = \omega^2 \mu_0 \varepsilon_2$, $C_m$, $D_m$, $G_r$, $F_r$ are constants.

The transverse field components can be expressed as

$$E_\xi = -\frac{j}{Q\chi^2}\left[\omega\mu_0 \frac{\partial H_z}{\partial \eta} + \beta \frac{\partial E_z}{\partial \xi}\right],$$
$$E_\eta = -\frac{j}{Q\chi^2}\left[-\omega\mu_0 \frac{\partial H_z}{\partial \xi} + \beta \frac{\partial E_z}{\partial \eta}\right],$$
$$H_\xi = -\frac{j}{Q\chi^2}\left[\beta \frac{\partial H_z}{\partial \xi} - \omega\varepsilon \frac{\partial E_z}{\partial \eta}\right], \tag{8}$$
$$H_\eta = -\frac{j}{Q\chi^2}\left[\beta \frac{\partial H_z}{\partial \eta} + \omega\varepsilon \frac{\partial E_z}{\partial \xi}\right]$$

where: $Q = q(\mathrm{sh}^2 \xi + \sin^2 \eta)^{1/2}$.

Using the boundary conditions for the tangential components of the field we obtain the set of equations to solve [9]. For a nontrivial solution, the determinant of the set of equations must be equal to zero. Thus, we obtain the characteristic equation, from which for given fiber parameters the propagation constant of the odd modes can be determined.

For example, the characteristic equation for $m = 1$ has the form of the infinite determinant equal to zero

$$\begin{vmatrix}
g_{1,1} & h_{1,1} & g_{3,1} & h_{3,1} & g_{5,1} & h_{5,1} & \cdots \\
t_{1,1} & s_{1,1} & t_{3,1} & s_{3,1} & t_{5,1} & s_{5,1} & \cdots \\
g_{1,3} & h_{1,3} & g_{3,3} & h_{3,3} & g_{5,3} & h_{5,3} & \cdots \\
t_{1,3} & s_{1,3} & t_{3,3} & s_{3,3} & t_{5,3} & s_{5,3} & \cdots \\
g_{1,5} & h_{1,5} & g_{3,5} & h_{3,5} & g_{5,5} & h_{5,5} & \cdots \\
t_{1,5} & s_{1,5} & t_{3,5} & s_{3,5} & t_{5,5} & s_{5,5} & \cdots \\
\cdot & \cdot & \cdot & \cdot & \cdot & \cdot & \\
\cdot & \cdot & \cdot & \cdot & \cdot & \cdot & \\
\cdot & \cdot & \cdot & \cdot & \cdot & \cdot &
\end{vmatrix} = 0 \tag{9}$$

where: $g$, $h$, $t$ and $s$ are defined in [9].

Practically, the determinant can be significantly reduced depending on a demanded accuracy. For the modes of the main number $m$, the first element of the determinant is $g_{m,m}$.

*Even ${}_{o}HE_{mp}$ and ${}_{e}EH_{mp}$ modes*

General expressions for the axial magnetic and electric fields of the even mode have a similar form to Eqs. (6), (7) when we replace in these equations the even Mathieu functions by the odd ones and vice versa. Using the boundary conditions, after transformations, we obtain the characteristic equation of the even modes in the form of the infinite determinant equal to zero [9].

*Approximate characteristic equations*

In the case of the weakly guiding fiber, *i.e.*, when $\Delta = (n_1 - n_2)/n_2 \ll 1$, where $n_1$ and $n_2$ are the core and cladding refractive indices, respectively, instead of the infinite determinant equal to zero (9), for the odd modes we obtain the characteristic equation in a form

$$\left[\frac{1}{\gamma_1^2}\frac{b'_m}{b_m} - \frac{1}{\gamma_2^2}\frac{p'_m}{p_m}\right]\left[\frac{n_1^2}{\gamma_1^2}\frac{a'_m}{a_m} - \frac{n_2^2}{\gamma_2^2}\frac{l'_m}{l_m}\right] = \frac{N^2 m^2}{(\gamma_1^2 B)^2} \tag{10}$$

where $B = (N^2 - n_2^2)/(n_1^2 - n_2^2)$ here denotes the relative propagation constant, $N = \beta/k$ is the normalized refractive index, $k$ is the wave-number of the free space, $a_m = \mathrm{Ce}_m(\xi_0)$, $b_m = \mathrm{Se}_m(\xi_0)$, $l_m = \mathrm{Fek}_m(\xi_0)$, $p_m = \mathrm{Gek}_m(\xi_0)$, and sign $'$ denotes a derivative of a function with respect to $\xi_0$.

Similarly as for the odd modes, we obtain the approximate characteristic equation for the even modes of weakly guiding fiber in the form of Eq. (10) when we replace in this equation the even Mathieu functions by the odd ones and vice versa [9].

The approximate characteristic equations are relatively simple and enable the exact estimation of the propagation constants difference of the modes in a weakly-guiding fiber.

*Classification of the modes*

There are two fundamental modes: odd ${}_{o}HE_{11}$ and even ${}_{e}HE_{11}$. Because of the difference between their propagation constants a structural birefringence appears and it is defined as

$$\Delta\beta = \beta_o - \beta_e \tag{11}$$

where: $\beta_o$ – propagation constant of the ${}_{o}HE_{11}$ mode, $\beta_e$ – propagation constant of the ${}_{e}HE_{11}$ mode. In the step-index elliptical fiber the higher-order modes are: ${}_{e}EH_{01}$, ${}_{e}HE_{01}$, ${}_{o}HE_{21}$, ${}_{e}HE_{21}$, ${}_{o}EH_{11}$, ${}_{e}EH_{11}$, ${}_{o}HE_{31}$, ${}_{e}HE_{31}$, ${}_{o}HE_{12}$, ${}_{e}HE_{12}$, ${}_{o}EH_{21}$, ${}_{e}EH_{21}$, ${}_{o}EH_{02}$, ${}_{e}HE_{02}$, ${}_{o}EH_{22}$, ${}_{e}HE_{22}$, ${}_{o}EH_{31}$, ${}_{e}EH_{31}$ .... . The circular hybrid HE (EH) modes correspond to the two modes HE (EH) in elliptical fiber, odd and even ones,

designated by prescripts "o" and "e", respectively. Instead of the axial symmetric modes $TE_{0p}$ and $TM_{0p}$ we have the hybrid modes ${}_eEK_{0p}$ and ${}_oEH_{0p}$, respectively.

*Numerical results*

The Fortran programs for the Mathieu functions which we use in our numerical computations are based on the algorithms that have been developed by YAMASHITA [18], [19]. The accuracy of the Mathieu functions is confirmed to be of more than ten significant digits for the double precision computations. It has been proved that a $4\times4$ determinant is sufficient to obtain the practically accurate values of propagation constants of the step-index fiber. Computations were carried out for the silica step-index elliptical fibers doped $GeO_2$ at the wavelength $\lambda = 1.3$ μm ($n_2 = 1.446917$).

In Figure 3, the propagation characteristics $B = f(V)$ of the odd ${}_oHE_{11}$ mode are shown, for $\Delta = 1\%$ and various values of $c = b/a$, where $B = (N^2-n_2^2)/(n_1^2-n_2^2)$ is the relative propagation constant, $V = ka(n_1^2-n_2^2)^{1/2}$ is the normalized frequency, $\Delta = (n_1-n_2)/n_2$, $N = \beta/k$. The propagation characteristics of the even fundamental mode are almost the same as for the odd one because their propagation constants differ slightly. Both fundamental modes have the cut-off frequency $V_c$ equal to zero.

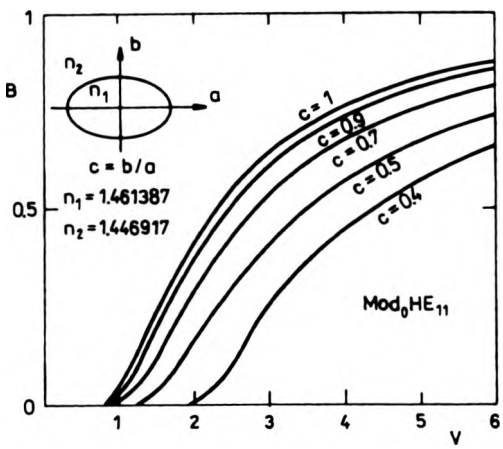


Fig. 3. Propagation characteristics $B = f(V)$ of the odd ${}_oHE_{11}$ mode for $\Delta = 1\%$ and various values of $c$.

The structural birefringence becomes larger as the relative index difference $\Delta$ and ellipticity of the core of a fiber $e = 1-b/a$ are increasing (Tab. 1). The step-index elliptical fiber of low-dispersion can realize the modal birefringence of value $B$ about $10^{-5}$.

The first higher mode of the step-index elliptical fiber is ${}_oEH_{01}$. Its normalized cut-off frequency

$$V_c = ka(n_1^2-n_2^2)^{1/2} \tag{12}$$

Table 1. Structural birefringence $\Delta\beta$ of the step-index elliptical fibers versus $V$ and $c$, for $\Delta = 1\%$

| | $\Delta\beta = \beta_e - \beta_o$ [1/m] | | | | | |
|---|---|---|---|---|---|---|
| $c$ \ $V$ | 1.8 | 2.2 | 2.6 | 3 | 3.5 | 4 |
| 0.9 | 35.64 | 34.53 | 30.39 | 25.76 | 20.58 | 16.42 |
| 0.7 | 109.45 | 119.09 | 112.74 | 100.49 | 83.98 | 69.18 |
| 0.5 | 154.14 | 204.20 | 220.10 | 214.96 | 195.10 | 170.77 |

can be calculated from the condition

$$Ce_0(\xi_0, \gamma^2) = 0$$

where $\gamma^2 = (k^2 n_1^2 - k^2 n_2^2)q^2/4$. It is greater than 2.405 and depends significantly on ellipticity of the fiber (Tab. 2). For small values of $c$ we have that $V_c \to 0.5\ \pi/c$.

Table 2. Normalized cut-off frequency of the ${}_eEH_{11}$ mode versus $c$

| $c$ | 0.9 | 0.8 | 0.7 | 0.6 | 0.5 |
|---|---|---|---|---|---|
| $V_c$ | 2.542 | 2.720 | 2.960 | 3.293 | 3.777 |

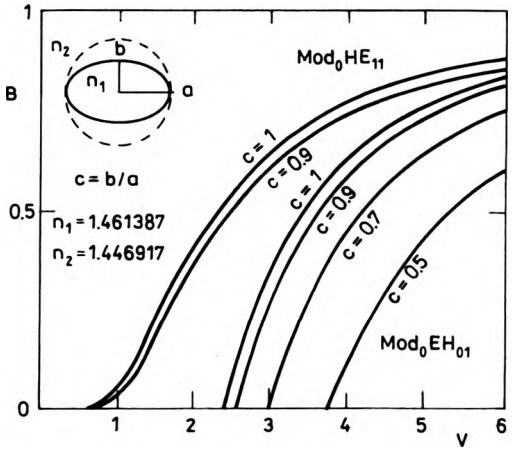


Fig. 4. Propagation characteristics $B = f(V)$ of the odd ${}_eHE_{11}$ and ${}_eEH_{01}$ modes for $\Delta = 1\%$ and various values of $c$.

Propagation characteristics of the first odd modes ${}_oHE_{11}$ and ${}_oEH_{01}$ for $\Delta =$ % and various values of the $c$ are shown in Fig. 4. The dispersion $D = -(1/f)\partial^2 N/\partial\lambda^2$ versus wavelength $\lambda$ of the odd fundamental mode ${}_oHE_{11}$ for parameters: $a = 3.2$ μm, $\Delta = 0.9\%$ is presented in Fig. 5. The dispersion characteristics of fundamental modes are practically the same but they are significantly different compared to those of the

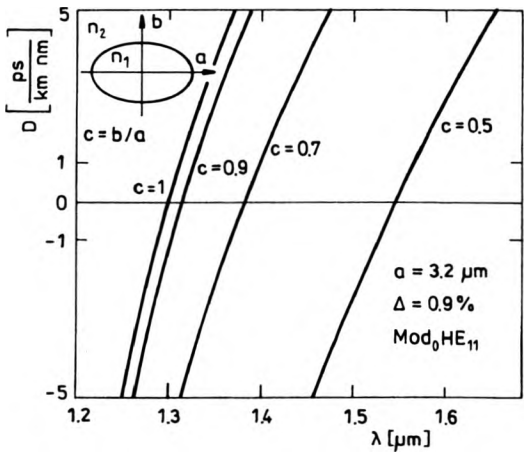


Fig. 5. Dispersion characteristics of ${}_{o}HE_{11}$ mode for odd $a = 3.2$ μm, $\Delta = 0.9\%$ and various values of $c$.

circular step-index fiber, *i.e.*, they are shifted towards long wavelength range. Changing the values of parameters $a$, $b$ and the index difference we can design fibers of the zero dispersion in the wavelength range $1.3-1.55$ μm.

## 2.2. Double-step confocal-elliptical fibers

The method described in Subsection 2.1. can be extended for the multistep-index confocal-elliptical fibers, particularly for the double-step fibers of refractive indices: $n_1$, $n_2$ and $n_3$, where $n_3 < \max(n_1, n_2)$, (Fig. 6). In this case, two elliptical cylinders, with $\xi = \xi_1$ and $\xi = \xi_2$, are assumed to coincide with the boundaries of the layers 1 and 2, respectively.

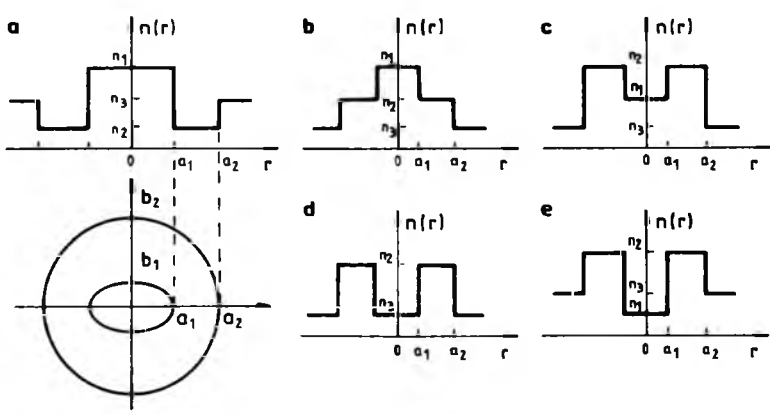


Fig. 6. Models of the double-step confocal-elliptical fibers.

### *Odd ${}_{o}HE_{mp}$ and ${}_{o}EH_{mp}$ modes*

The axial magnetic and electric fields of odd modes can be expressed as follows:

$$H_{z1} = \sum_{m=1}^{\infty} B_m^{(1)} Se_m(\xi, \gamma_1^2) se_m(\eta, \gamma_1^2),$$
$$E_{z1} = \sum_{m=0}^{\infty} A_m^{(1)} Ce_m(\xi, \gamma_1^2) ce_m(\eta, \gamma_1^2) \tag{13}$$

for layer 1,

$$H_{z2} = \sum_{m=1}^{\infty} B_m^{(2)} G_m(\xi, \gamma_2^2) se_m(\eta, \gamma_2^2),$$
$$E_{z2} = \sum_{m=0}^{\infty} A_m^{(2)} F_m(\xi, \gamma_2^2) ce_m(\eta, \gamma_2^2) \tag{14}$$

for layer 2,

$$H_{z3} = \sum_{m=1}^{\infty} B_m^{(3)} Gek_m(\xi, \gamma_3^2) se_m(\eta, \gamma_3^2),$$
$$E_{z3} = \sum_{m=0}^{\infty} A_m^{(3)} Fek_m(\xi, \gamma_3^2) ce_m(\eta, \gamma_3^2) \tag{15}$$

for layer 3 (cladding), where $\gamma_i^2 = (k_i^2 - \beta^2)q^2/4$, $k_i^2 = k^2 n_i^2$, $i = \{1, 2, 3\}$, $q$ is the semifocal length, $n_i$ is the refractive index for layer of number $i$, $A_m^{(i)}$, $B_m^{(i)}$ are the constants.

The field equations in layer 2 depend on the refractive-index profile of the fiber. For the model, which corresponds to the well known circular $W$ profile (Fig. 6a), we have the following expressions:

$$F_m(\xi, \gamma_2^2) = Ce(\xi, \gamma_2^2) + [C_m^{(2)}/A_m^{(2)}] Fek_m(\xi, \gamma_2^2),$$
$$G_m(\xi, \gamma_2^2) = Se(\xi, \gamma_2^2) + [D_m^{(2)}/B_m^{(2)}] Gek_m(\xi, \gamma_2^2), \tag{16}$$

and for the models shown in Fig. 6c–e:

$$F_m(\xi, \gamma_2^2) = Ce(\xi, \gamma_2^2) + [C_m^{(2)}/A_m^{(2)}] Fey_m(\xi, \gamma_2^2),$$
$$G_m(\xi, \gamma_2^2) = Se(\xi, \gamma_2^2) + [D_m^{(2)}/B_m^{(2)}] Gey_m(\xi, \gamma_2^2) \tag{17}$$

where $C_m^{(2)}$ and $D_m^{(2)}$ are the arbitrary constants. For the model in Fig. 6b either expression (16) or (17) are used depending on the value of $\gamma_2^2$.

Using the boundary conditions for the tangential components of the field we obtain the set of equations and finally the characteristic equation of the odd modes in the form of the infinite determinant equal to zero [9].

*Odd ${}_oHE_{mp}$ and ${}_oEH_{mp}$ modes*

The axial magnetic and electric fields of odd modes can be expressed in a similar form to Eqs. (13)–(15) when we replace in these equations the even Mathieu functions by the odd ones and vice versa [9]. The characteristic equation in this case has a similar form like for odd modes when we replace in the determinant elements the variables and even Mathieu functions by the odd ones and vice versa [9].

Similarly to the case of the step-index elliptical fibers (Subsec. 2.1), we can obtain the approximate characteristic equation for the modes of the double-step weakly guiding fiber [9].

*Numerical results*

It has been proved numerically that the elliptical fibers preserve the polarization and show the properties of circular fibers [20]. Results are presented for the silica double-step elliptical fiber of $W$ profile (Fig. 6a) doped with $GeO_2$ and F, respectively, for the wavelength $\lambda = 1.3$ μm. The complete set of characteristics for the other profiles of fibers, shown in Fig. 6, is given in [9]. Sufficient accuracy of the propagation constant calculation was obtained for a $4 \times 4$ determinant of the characteristic equation. The relative propagation constant $B = (N^2 - n_3^2)/(n_1^2 - n_3^2)$ versus normalized frequency $V = ka_1(n_1^2 - n_3^2)^{1/2}$ of the fundamental mode ${}_eHE_{11}$, for given $\Delta_i = (n_i - n_3)/n_3$, $i = \{1, 2\}$, and selected values of $d = b_1/a_1$, is presented in Fig. 7.

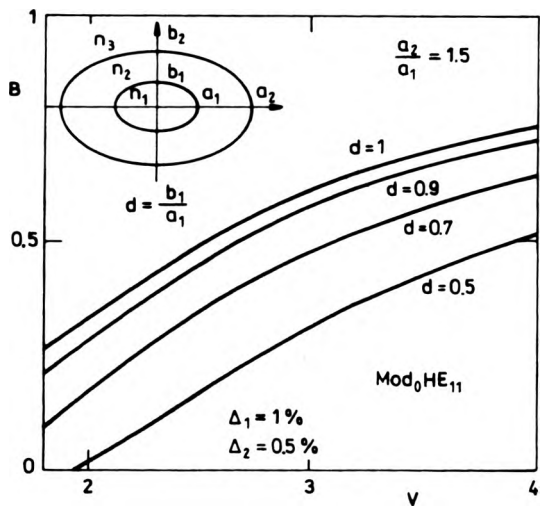


Fig. 7. Propagation characteristics $B = f(V, d)$ of the odd ${}_eHE_{11}$ mode for fibers as shown in Fig. 6a.

In Table 3, the dependence of the structural birefringence on the normalized frequency $V$ is presented. It is possible to get the larger structural birefringence than that of the step-index elliptical fiber even in the case of small ellipticity (300 – 500 [1/m]). When we increase the ellipticity $e$, the structural birefringence becomes larger (up to 1000 [1/m]). It can be larger than 2000 [1/m] that corresponds to $B$ of $4 \times 10^{-4}$ when the concentrations of dopants are appropriate higher. So, we can get the similar values of $B$ like in the case of anisotropic silica fibers Bow-Tie and Panda, in which the birefringence arises from high mechanical stresses.

When the value of $c$ is large enough, the fundamental modes have the cut-off frequency $V > 0$. The cut-off characteristics of the odd fundamental and the higher-order modes: ${}_eEH_{11}$ and ${}_eHE_{01}$ are shown in Figs. 8 and 9, respectively, where $y = (n_1^2 - n_2^2)/(n_1^2 - n_3^2)$.

Table 3. Structural birefringence $\Delta\beta$ of the fibers as shown in Fig. 6a versus $V$ for various values of semi-axes ratios, $\Delta_1 = 1.4721\%$ ($GeO_2$ – 3.5 M%), $\Delta_2 = -0.6082\%$ (F – 2 M%)

– for the case: $a_2/a_1 = 1.25$

| | $\Delta\beta = \beta_o - \beta_e$ [1/m] | | | | | | |
|---|---|---|---|---|---|---|---|
| $d$ \ $V$ | 2 | 2.25 | 2.5 | 2.75 | 3 | 3.25 | 3.5 |
| 0.9 | 114.83 | 110.17 | 101.53 | 91.55 | 81.60 | 72.33 | 63.96 |
| 0.7 | 383.79 | 398.24 | 387.11 | 362.72 | 332.79 | 301.64 | 271.56 |
| 0.5 | 523.08 | 678.12 | 755.44 | 775.09 | 758.64 | 721.93 | 675.15 |

– for the case: $a_2/a_1 = 1.5$

| | $\Delta\beta = \beta_o - \beta_e$ [1/m] | | | | | | |
|---|---|---|---|---|---|---|---|
| $d$ \ $V$ | 2 | 2.25 | 2.5 | 2.75 | 3 | 3.25 | 3.5 |
| 0.9 | 129.12 | 121.38 | 109.73 | 97.36 | 85.67 | 75.16 | 65.94 |
| 0.7 | 435.37 | 444.23 | 422.41 | 388.23 | 350.75 | 314.18 | 280.32 |
| 0.5 | 517.57 | 768.52 | 850.42 | 850.71 | 813.72 | 760.70 | 702.14 |

– for the case: $a_2/a_1 = 5$

| | $\Delta\beta = \beta_o - \beta_e$ [1/m] | | | | | | |
|---|---|---|---|---|---|---|---|
| $d$ \ $V$ | 2.15 | 2.25 | 2.5 | 2.75 | 3 | 3.25 | 3.5 |
| 0,9 | 134.35 | 128.33 | 113.29 | 99.22 | 86.65 | 75.69 | 66.22 |
| 0.7 | 494.88 | 481.20 | 440.86 | 397.61 | 355.62 | 316.76 | 281.71 |
| 0.5 | 952.14 | 956.02 | 937.17 | 892.28 | 834.27 | 771.16 | 707.61 |

The dispersion characteristics of the fundamental modes: ${}_oHE_{11}$ and ${}_eHE_{11}$ for $W$ profile elliptical fiber of large relative-index difference are shown in Fig. 10, while the flattened dispersion characteristics of the odd mode ${}_oHE_{11}$ are given in Fig. 11.

The $W$ profile elliptical fiber, as shown in Fig. 6a, provides large value of the birefringence and has good propagation characteristics. Moreover, the mechanical stresses of the presented structure are not so high as in the case of Panda and Bow-Tie fibers, doped $B_2O_3$.

### 2.3. Triple-step confocal-elliptical fiber

The triple-step confocal-elliptical fiber (Fig. 12) has better dispersion characteristic (Fig. 13) than the fiber shown in Fig. 6a. Introducing the additional layer causes that the structural birefringence is slightly less compared to that of the double-step-index fiber with the same parameters (Tab. 4).

In Figure 14, the propagation characteristics of the first odd modes, *i.e.*, fundamental ${}_oHE_{11}$ mode and first higher ${}_oHE_{12}$ mode are presented for selected parameters of the fiber, where $\Delta_i = (n_i - n_4)/n_4$, $i = \{1, 2, 3\}$. The cut-off wavelength $\lambda_g$ becomes greater when $\Delta_3$ is increasing [9].

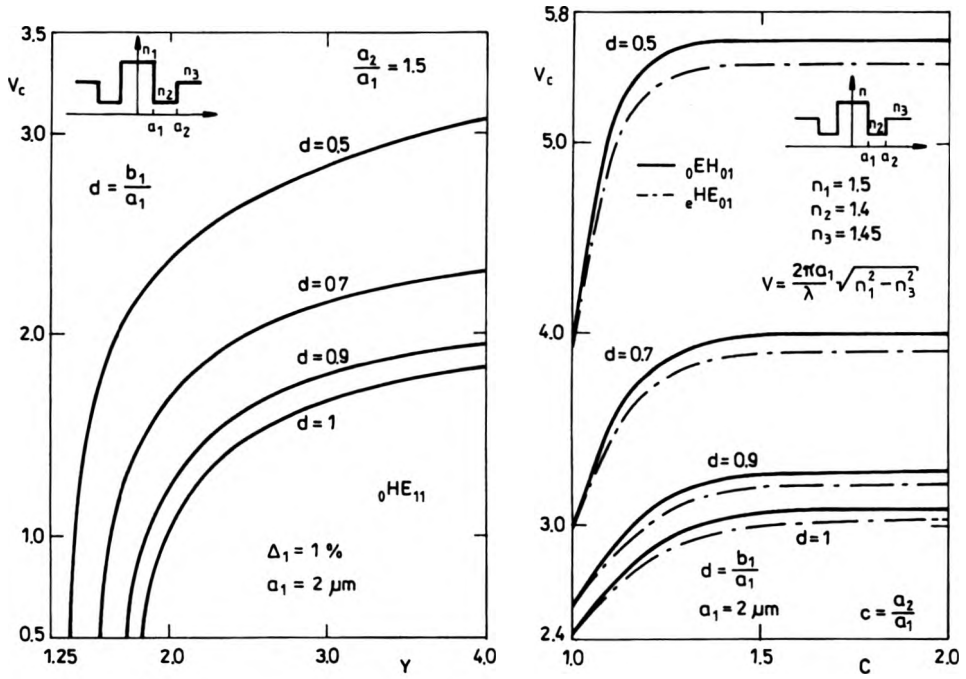


▲

Fig. 8. Dependence $V_c = f(y, d)$ of the $_eHE_{11}$ mode for fibers as shown in Fig. 6a.

Fig. 9. Dependence $V_c = f(c, d)$ of the $_eEH_{11}$ and $_eHE_{01}$ modes for fibers as shown in Fig. 6a.

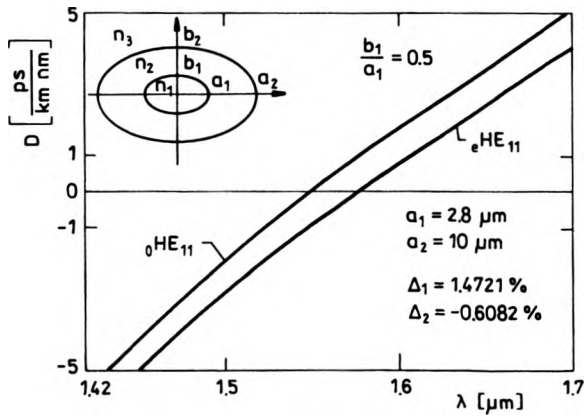


Fig. 10. Dispersion characteristics of the fundamental modes: $_0HE_{11}$ and $_eHE_{11}$ for the fiber as shown in Fig. 6a, when the structural birefringence is approximately equal to 750 [1/m].

From numerical analysis of the multi-step confocal-elliptical fibers, we can conclude that they have similar propagation properties as appropriate circular fibers and the structural birefringence depends mainly on the refractive-index difference in

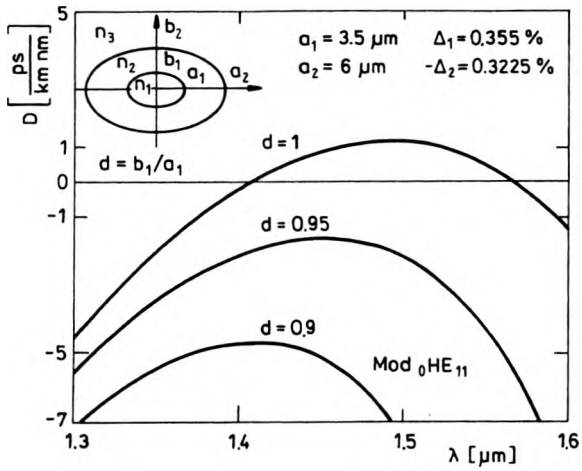


Fig. 11. Flattened dispersion characteristics of the fundamental mode $_{e}HE_{11}$ for the fiber as shown in Fig. 6a.

Table 4. Structural birefringence $\Delta\beta$ of the fibers as shown in Fig. 12 for $V = 2.75$, $b_1/a_1 = 0.5$, $a_2/a_1 = 1.5$, $\Delta_1 = 1.4721\%$ ($GeO_2$ – 3.5 M%), $\Delta_2 = -0.6082\%$ (F – 2 M%)

| | $\Delta\beta = \beta_o - \beta_e$ [1/m] | | |
|---|---|---|---|
| $a_3/a_1$ \ $\Delta_3$ | 0.1% | 0.3% | 0.5% |
| 2 | 828.97 | 807.00 | 778.48 |
| 3 | 823.37 | 770.86 | 621.48 |
| 5 | 822.34 | 746.35 | 187.29 |

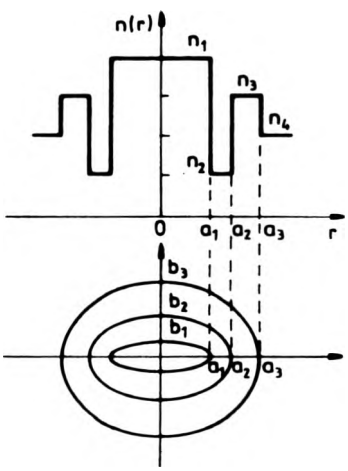


Fig. 12. Triple-step confocal-elliptical fiber.

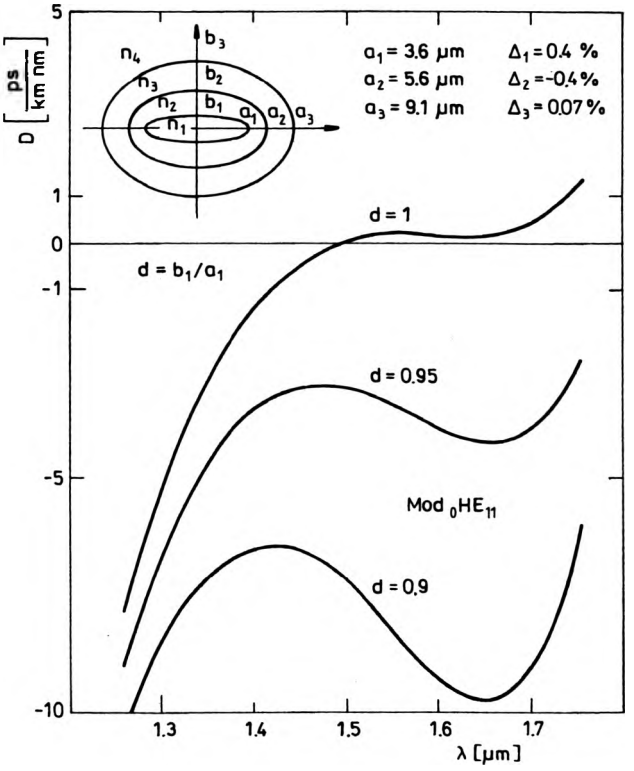


Fig. 13. Dispersion characteristics of the fundamental mode ${}_0HE_{11}$ for the fiber as shown in Fig. 12.

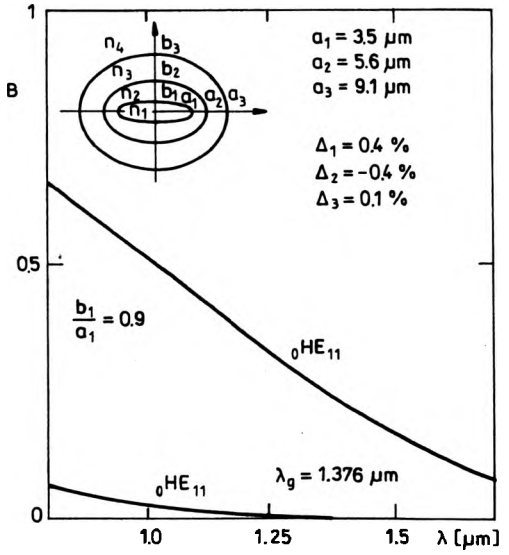


Fig. 14. Phase characteristics $B = f(\lambda)$ of the odd ${}_oHE_{11}$ and ${}_oHE_{12}$ modes for the fiber as shown in Fig. 12.

the first two layers. Moreover, the dispersion is very sensitive to small changes in geometry of the fiber. Therefore, the $W$ profile elliptical fiber seems to be optimal because of large birefringence, low dispersion and relatively simple structure.

## 3. Three-layer nonconfocal-elliptical fibers

The cross-sections of the $W$-type nonconfocal-elliptical fibers for two configurations: coaxial (**a**) and noncoaxial (**b**), are shown in Fig. 15. In order to investigate the three-layer elliptical fibers with layers of any ellipticity $e_j = 1 - b_j/a_j$, where $j = \{1, 2\}$, we apply the IPMM with Mathieu function expansion [10]. The noncoaxial structures of $W$-type circular fibers have been investigated by IPMM with Bessel function expansion, whose numerical results are quite reliable [21].

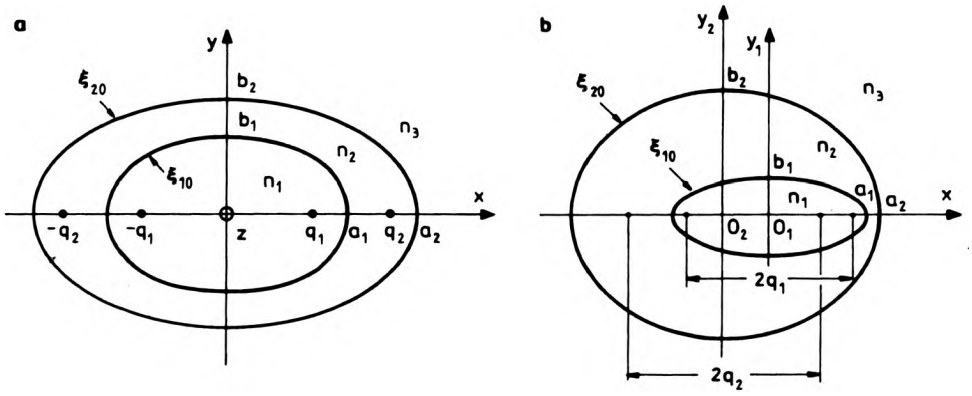


Fig. 15. Cross-section of the $W$-type nonconfocal-elliptical fibers for two configurations: **a** — coaxial and **b** — noncoaxial.

In the IPMM two elliptical coordinate systems $(\xi_1, \eta_1, z)$ and $(\xi_2, \eta_2, z)$ are introduced for the complete modal expansions and two of the elliptical cylinders with $\xi_1 = \xi_{10}$ and $\xi_2 = \xi_{20}$ are assumed to coincide with the boundaries of the layers 1 and 2, respectively. The propagation factor $e^{j(\omega t - \beta z)}$ ($\beta$ is the propagation constant in the $z$-direction and $\omega$ is the angular frequency) will be omitted in the expressions for the field components. Since the fiber structure is symmetrical about the $x$-axis, the electromagnetic fields can be separated into the odd modes ${}_{o}\mathrm{HE}_{mp}$, ${}_{o}\mathrm{EH}_{mp}$ and the even modes ${}_{e}\mathrm{HE}_{mp}$, ${}_{e}\mathrm{EH}_{mp}$. In our IPMM the $z$-components of electric and magnetic fields ($E_z$ and $H_z$) for the odd modes are approximated by the complete modal expansions with the Mathieu functions as follows:

$$H_{z1} = \sum_{n=1}^{N-1} \mathrm{B}_n^{(1)} \mathrm{Se}_n(\xi_1, \gamma_1^2)\, \mathrm{se}_n(\eta_1, \gamma_1^2), \qquad E_{z1} = \sum_{n=0}^{N-1} \mathrm{A}_n^{(1)} \mathrm{Ce}_n(\xi_1 \gamma_1^2)\, \mathrm{ce}_n(\eta_1, \gamma_1^2) \quad (18)$$

for layer 1,

$$H_{z2} = \sum_{l=1}^{L-1} B_l^{(2)} \mathrm{Se}_l(\xi_2, \gamma_{22}^2)\,\mathrm{se}_l(\eta_2, \gamma_{22}^2) + \sum_{n=1}^{N-1} D_n^{(2)} \mathrm{Gek}_n(\xi_1, \gamma_{21}^2)\,\mathrm{se}_n(\eta_1, \gamma_{21}^2),$$
$$E_{z2} = \sum_{l=0}^{L-1} A_l^{(2)} \mathrm{Ce}_l(\xi_2, \gamma_{22}^2)\,\mathrm{ce}_l(\eta_2, \gamma_{22}^2) + \sum_{n=0}^{N-1} C_n^{(2)} \mathrm{Fek}_n(_1, \gamma_{21}^2)\,\mathrm{ce}_n(\eta_1, \gamma_{21}^2) \tag{19}$$

for layer 2,

$$H_{z3} = \sum_{l=1}^{L-1} B_l^{(3)} \mathrm{Gek}_l(\xi_2, \gamma_3^2)\,\mathrm{se}_l(\eta_2, \gamma_3^2),$$
$$E_{z3} = \sum_{l=0}^{L=1} A_l^{(3)} \mathrm{Fek}_l(\xi_2, \gamma_3^2)\,\mathrm{ce}_l(\eta_2, \gamma_3^2), \tag{20}$$

for cladding, where $\gamma_1^2 = (k_1^2 - \beta^2)q_1^2/4$, $\gamma_{2j}^2 = (k_2^2 - \beta^2)q_j^2/4$, $\gamma_3^2 = (k_3^2 - \beta^2)q_2^2/4$, and $k_i = kn_i$, $q_j$ is the semifocal length in elliptical coordinate system of a number $j$, $j = \{1, 2\}$; ce, se are the even and odd Mathieu functions of the first kind; Ce, Se are even and odd modified Mathieu functions of the first kind; Fek, Gek are the even and odd modified functions of the second kind; $A_n^{(1)} \sim B_l^{(3)}$ are constants; $N$ and $L$ are the number of space harmonics taken in our IPMM. Axial field components for the even modes are in the form of Eqs. (18)–(20), when the even Mathieu functions are replaced by the odd ones and vice versa. The total transverse components of the field in layer 2 can be expressed by combining the fractional $\eta$-component and $\xi$-component in two elliptical coordinate systems at any points at $\xi_{10}$ and $\xi_{20}$ [10].

Because of the symmetry of the structure, the matching is only performed in the first quadrant of the $x-y$ plane (coaxial structures as shown in Fig. 15**a**) or the upper half of the $x-y$ plane (noncoaxial structures as shown in Fig. 15**b**), [13], [14].

Using the boundary conditions at equiangularly spaced points around the boundaries between layers of the fiber ($\xi_{10}$:$N$ points, $\xi_{20}$:$L$ points) yields finally the characteristic equation, from which we can get the propagation constants of the modes [10].

*Numerical results*

Numerical computations were carried out by using the truncation number $N = L$, which makes the relative error of the modal birefringence $B$ less than 0.01% [10]. The birefringence that arises from stress is assumed to be neglected in our considerations.

In our IPMM, unlike in the previously reported methods [11], [12], high computational accuracy was achieved even in the case of fibers with layers of larger ellipticity $e_j [= 1 - b_j/a_j$, $b_j$, $a_j$ – the semiaxes of elliptical layers, $j = \{1, 2\}]$.

Among the elliptical structures presented in this paper, the largest value of birefringence is realized by the fibers with hollow layers outside an elliptical core and $n_2 = 1$ (Fig. 16). It is possible to obtain the modal birefringence $B > 10^{-3}$ [13], *i.e.*, larger than for anizotropic fibers. The noncoaxial elliptical fibers (Fig. 16**c**) can realize the larger modal birefringence compared to the elliptical fibers with coaxial

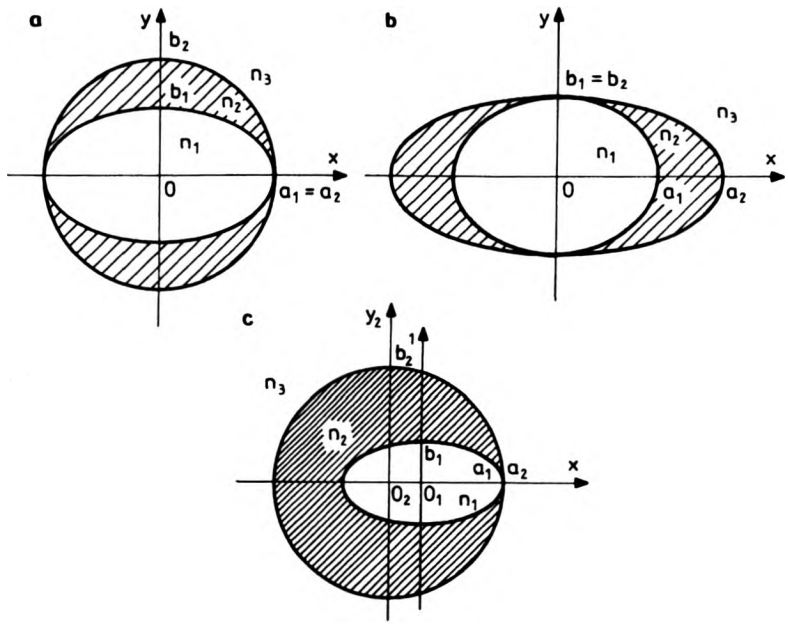


Fig. 16. Models of *W*-type elliptical fibers with hollow layers.

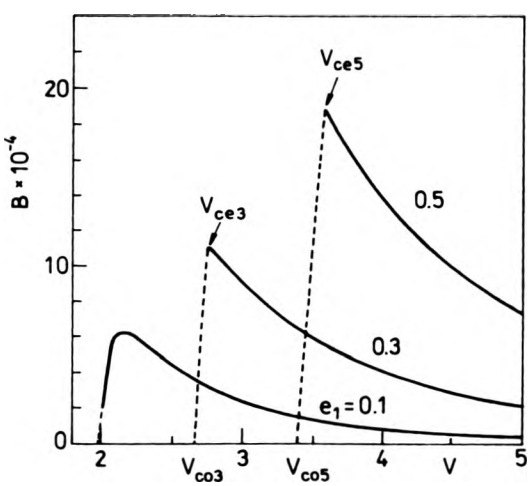


Fig. 17. Dependence of the modal birefringence $B$ on the normalized frequency $V$ for the elliptical fibers with a hollow layer and $a_1 = a_2$ (Fig. 16a) for different values of $e_1$, $e_2 = 0$ and $\Delta_1 = 1.4692\%$.

symmetry but they seem to be much more complicated to manufacture than symmetrical ones [22].

Our computations were carried out for the selected structures of the pure silica fibers as shown in Fig. 16 with hollow layers outside the germanium dioxide elliptical core ($\lambda = 1.3$ μm). Figure 17 shows the dependence of the modal birefringence $B$

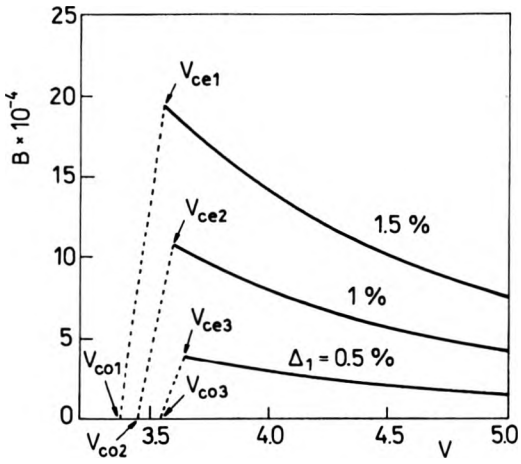


Fig. 18. Dependence of the modal birefringence $B$ on the normalized frequency $V$ for the elliptical fibers with a hollow layer and $a_1 = a_2$ (Fig. 16a) for different values of $\Delta_1$, $e_1 = 0.5$ and $e_2 = 0$.

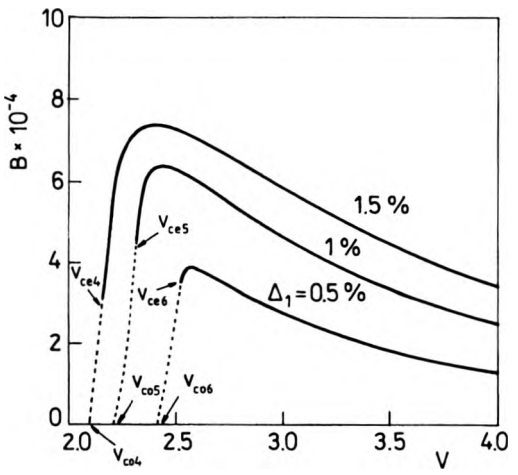


Fig. 19. Dependence of the modal birefringence $B$ on the normalized frequency $V$ for the elliptical fibers with a hollow layer and $b_1 = b_2$ (Fig. 16b) for different values of $\Delta_1$, $e_1 = 0.3$ and $e_2 = 0.5$.

on the normalized frequency $V = ka_1(n_1^2 - n_3^2)^{1/2}$ for the first group of the elliptical fibers with a hollow layer and $a_1 = a_2$ (Fig. 16a) for different values of $e_1$, $e_2 = 0$ and $\Delta_1 = 1.4692\%$.

The modal birefringence $B$ versus normalized frequency $V$ for fibers representing the second group of the fibers with symmetry and $a_1 = a_2$ (Fig. 16a) for different values of $\Delta_1$, $e_1 = 0.5$ and $e_2 = 0$ is given in Fig. 18. In the frequency range $V_{cor} < V < V_{cer}$ (broken-line curves in Fig. 18), the single-mode single-polarization transmission is possible, where $r = 1 \ldots 6$; $V_{cor}$ and $V_{cer}$ denote the normalized cut-off frequencies of the odd and even fundamental modes, respectively, and we

have that: $V_{ce1} \simeq 3.55$, $V_{co1} \simeq 3.37$, $V_{ce2} \simeq 3.59$, $V_{co2} \simeq 3.45$, $V_{ce3} \simeq 3.65$, $V_{co3} \simeq 3.54$, $V_{ce4} \simeq 2.15$, $V_{co4} \simeq 2.06$, $V_{ce5} \simeq 2.31$, $V_{co5} \simeq 2.20$, $V_{ce6} \simeq 2.52$, $V_{co6} \simeq 2.41$.

The modal birefringence $B$ versus normalized frequency $V$ for fibers representing the second group of the fibers with symmetry and $b_1 = b_2$ (Fig. 16b) for different values of $\Delta_1$, $e_1 = 0.3$ and $e_2 = 0.5$ is given in Fig. 19. By changing the value of parameters we can design the optimal shape of modal birefringence characteristics.

## 4. Conclusions

The analysis of isotropic multi-step optical-fiber structures with elliptical geometry, in particular the fiber structures which provide the large value of the birefringence has been presented.

As the first group of fibers we investigate the following confocal multi-layer structures: the step-index elliptical fiber, double-step confocal-elliptical fibers and triple-step confocal elliptical fiber. The multi-layer confocal-elliptical fibers can be analyzed by the exact analytical method with Mathieu function expansion and characteristic equations for the modes have the form of infinite determinants equal to zero. In that group of fibers, the fibers of the $W$-profile provide the largest value of the modal birefringence $B$ (about $10^{-4}$ and even more).

The second group of elliptical fibers are three-layer nonconfocal elliptical fibers, *i.e.*, the fibers with layers of any ellipticity. In order to investigate the three-layer nonconfocal elliptical fibers we apply the improved point-matching method and the electromagnetic field components are expressed by the complete modal expansions with the Mathieu functions. In particular, we discuss the optical fibers with hollow layers outside an elliptical core, which provide the very large value of the modal birefringence $B$ (about $10^{-3}$). In the case of such structures, it is possible to obtain the non-zero cut-off frequency of the even fundamental mode and they can be suitable for the single-mode single-polarization transmission.

### References

[1] LUBIMOV L. A., VESELOV N. A., BEJ N. A., Radiotechn. Elektron. (in Russian) **6** (1961), 1871.
[2] YEH C., J. Appl. Phys. **33** (1962), 3235.
[3] YEH C., Opt. Quantum Electron. **8** (1976), 43.
[4] YEH C., IEEE Trans. AP **11** (1963), 177.
[5] DYOTT R. B., COZENS J. R., MORRIS D. G., Electron. Lett. **15** (1979), 380.
[6] RENGARAJAN S. R., LEWIS J. E., Electron. Lett. **16** (1980), 263.
[7] LEWIS J. E., DESHPANDE G., IEE J. Microwaves, Opt. Acous. **3** (1979), 147.
[8] RENGARAJAN S. R., LEWIS J. E., Radio Sci. **16** (1981), 541.
[9] KRASIŃSKI Z., MAJEWSKI A., *Analiza numeryczna jednomodowych światłowodów eliptycznych* (in Polish), Wyd. PW, E. 94, 1991.
[10] KRASIŃSKI Z., MAJEWSKI A., HINATA T., Opto-Electron. Rev., No. 4 (1993), 111.
[11] YAMASHITA E., ATSUKI K., NISHINO Y., IEEE Trans. MTT **29** (1981), 987.
[12] MIYAMOTO T., IEE Proc. J. **38** (1991), 1.
[13] KRASIŃSKI Z., HINATA T., YAMASHITA S., MAJEWSKI A., IEICE Trans. Electron. Jpn. E **78-C** (1995), 111.

[14] MC LACHLAN N. W., *Theory and Application of Mathieu Functions*, Oxford at the Clarendon Press, 1947.
[15] BARK S., DIMITRIIEVA I., ZAKHAREV N., *Tablitsy sobstvennykh znachenii upraveniaya Matie*, (in Russian), Moscow, 1970.
[16] VZIATYSHEV V. F., *Dielektricheskiie volnovody* (in Russian), [Ed.] Sov. Radio, Moscow, 1970.
[17] MAJEWSKI A., OWCZAREK L., *Graficzna interpretacja modów światłowodu włóknistego* (in Polish), Wyd. PW, E. **102** (1993).
[18] YAMASHITA S., Trans. IPS Jpn. **33** (1992), 1290.
[19] YAMASHITA S., Trans. IPS Jpn. **34** (1993), 191.
[20] MAJEWSKI A., *Teoria i projektowanie światłowodów* (in Polish), [Ed.] WNT, Warszawa 1991.
[21] HOSONO T., HINATA T., YOSHIKAWA H., Radio Sci. **19** (1984), 1265.
[22] KRASIŃSKI Z., MAJEWSKI A., HINATA T., Bull. Polish Acad. Sci. **45** (1997), 137.

*Received February 8, 1999*